AKT Ser/Thr kinase increases V-ATPase–dependent lysosomal acidification in response to amino acid starvation in mammalian cells

Received for publication, February 25, 2020, and in revised form, May 13, 2020 Published, Papers in Press, May 14, 2020, DOI 10.1074/jbc.RA120.013223

Michael P. Collins[1], **Laura A. Stransky**[2], **and Michael Forgac**[1,2,3,*]

From the [1]*Program in Cell, Molecular and Developmental Biology and* [2]*Program in Cellular and Molecular Physiology, Tufts University Graduate School of Biomedical Sciences, Boston, Massachusetts, USA, and the* [3]*Department of Developmental, Molecular, and Chemical Biology, Tufts University School of Medicine, Boston, Massachusetts, USA*

Edited by Phyllis I. Hanson

The vacuolar H^+-ATPase (V-ATPase) is an ATP-dependent proton pump that is essential for cellular homeostasis. V-ATPase activity is controlled by the regulated assembly of the enzyme from its component V_1 and V_0 domains. We previously reported that amino acid starvation rapidly increases V-ATPase assembly and activity in mammalian lysosomes, but the signaling pathways controlling this effect are unknown. In testing inhibitors of pathways important for controlling cellular metabolism, we found here that the cAMP-dependent protein kinase (PKA) inhibitor H89 increases lysosomal V-ATPase activity and blocks any further change upon starvation. The AMP-activated protein kinase (AMPK) inhibitor dorsomorphin decreased lysosomal V-ATPase activity and also blocked any increase upon starvation. However, CRISPR-mediated gene editing revealed that PKA and AMPK are not required for the starvation-dependent increase in lysosomal V-ATPase activity, indicating that H89 and dorsomorphin modify V-ATPase activity through other cellular targets. We next found that the AKT Ser/Thr kinase (AKT) inhibitor MK2206 blocks the starvation-dependent increase in lysosomal V-ATPase activity without altering basal activity. Expression of AKT1 or AKT3, but not AKT2, was required for increased lysosomal V-ATPase activity in response to amino acid starvation in mouse fibroblasts. Finally, HEK293T cells expressing only AKT1 responded normally to starvation, whereas cells expressing only AKT2 displayed a significantly reduced increase in V-ATPase activity and assembly upon starvation. These results show that AKT is required for controlling the rapid response of lysosomal V-ATPase activity to changes in amino acid availability and that this response depends on specific AKT isoforms.

Amino acid homeostasis, which involves balancing the production and utilization of free amino acids, is essential to cellular and organismal viability. To achieve homeostasis, cells must continually sense amino acid availability and respond accordingly. A major way that cells replenish the available supply of amino acids is through lysosomal proteolysis, which depends upon the low lumenal pH generated by vacuolar H^+-ATPase (V-ATPase). The V-ATPase is an ATP-dependent proton pump that functions to transport protons from the cytosol into various intracellular compartments or across the plasma membrane of specialized cells (1–4). V-ATPase–dependent acidification is essential for a variety of cellular processes. Acidification of early endosomes promotes ligand/receptor dissociation, which is important for signal termination and receptor recycling (5). Similarly, acidification of late endosomes causes dissociation of lysosomal proteases from mannose 6-phosphate receptors as they are trafficked to the lysosome (6). The formation of endosomal carrier vesicles is also pH-dependent, as is autophagosome/lysosome fusion (7, 8). Degradation of lysosomal contents depends on the activation of acid-dependent proteases. Finally, the proton gradient generated by the V-ATPase drives the coupled transport of small molecules, such as amino acids, out of the lysosome (9). Because these various processes occur within discrete pH ranges, the activity of the V-ATPase is highly regulated.

The V-ATPase is composed of two multisubunit domains: the peripheral V_1 domain that hydrolyzes ATP and the integral V_0 domain that transports protons (1, 2). V-ATPase activity is controlled by reversible dissociation of the V_1 and V_0 domains, a process termed regulated assembly, where both the catalytic and transport functions of the enzyme are inhibited upon disassembly (1, 4, 10). Regulated assembly has been best characterized in yeast, where glucose deprivation rapidly lowers assembly in order to preserve energy (4, 10, 11). We showed this process is controlled by the Ras/cAMP/PKA pathway, where hyperactivation of the pathway causes the V-ATPase to remain assembled even upon glucose starvation (12). Regulated assembly also occurs in mammalian cells, but the stimuli and signaling pathways controlling it are not the same as those in yeast. In mammalian cells, elevated glucose causes increased V-ATPase assembly and activity via the phosphoinositide-3-kinase (PI3K)/AKT pathway (13). Moreover, we recently reported that acute glucose starvation also increases V-ATPase assembly and lysosomal activity in mammalian cells, and that inhibitors of PI3K/AKT and AMPK block this effect (14). This was the first demonstration of AMPK control of assembly in any system, while PI3K is known to be important for increasing assembly in cells infected with influenza virus and in dendritic cells upon maturation (15, 16). V-ATPase assembly and activity also respond to changes in amino acid availability, with amino acid starvation causing increased

* For correspondence: Michael Forgac, michael.forgac@tufts.edu.
Present address for Laura A. Stransky: Department of Medical Oncology, Dana-Farber Cancer Institute, Boston, Massachusetts, USA.

assembly and lysosomal acidification (17). Interestingly, unlike the examples discussed above, inhibition of either PI3K or one of its major effectors, mTOR complex 1 (mTORC1), failed to block the increase in assembly and lysosomal acidification upon amino acid starvation (17).

In the present study, we sought to identify the pathways controlling V-ATPase–dependent lysosomal acidification in response to amino acid starvation. Using a combination of pharmacological and genetic approaches, we find that the PKA inhibitor H89 and the AMPK inhibitor dorsomorphin alter V-ATPase-dependent lysosomal acidification through off-target effects. In contrast, results using the AKT inhibitor MK2206 and genetic analysis demonstrate that AKT is important for controlling lysosomal V-ATPase activity upon amino acid starvation. AKT, also known as protein kinase B (PKB), is a serine/threonine kinase with diverse substrates that functions to promote survival, growth, and other anabolic processes (18). We now report that AKT1 or AKT3, but not AKT2, is required for the increase in V-ATPase–dependent lysosomal acidification in response to amino acid withdrawal.

Results

PKA and AMPK inhibitors modulate lysosomal V-ATPase activity in the presence and absence of amino acids

We previously reported that in mammalian cells, amino acid starvation increases V-ATPase assembly and lysosomal V-ATPase activity independently of PI3K or its major effector, mTORC1 (17). Because previous studies have suggested the involvement of PKA and AMPK in modulating V-ATPase activity (12, 14, 19, 20), we wished to test the involvement of these important signaling pathways in controlling the starvation-dependent increase in lysosomal V-ATPase activity. To test the role of the PKA pathway, we first determined the minimum concentration of the PKA inhibitor H89 necessary to inhibit forskolin-induced, PKA-dependent phosphorylation of vasodilator-stimulated phosphoprotein (VASP) (21) in HEK293T cells. As shown in Fig. 1*A*, 50 μM H89 completely inhibits PKA activity. We next tested the effect of H89 on lysosomal V-ATPase activity in HEK293T cells maintained in amino acids or starved for 1 h. As shown in Fig. 1*B*, H89 significantly increases basal lysosomal V-ATPase activity and blocks any further changes to activity upon amino acid starvation. This suggested that PKA is important for controlling the steady-state level of lysosomal V-ATPase activity in mammalian cells and, possibly, the response to amino acid starvation.

To test the involvement of the AMPK pathway, we first determined the minimum concentration of the AMPK inhibitor dorsomorphin necessary to inhibit AMPK in HEK293T cells, as measured by phosphorylation of the AMPK substrate acetyl-CoA carboxylase (ACC) (22). As shown in Fig. 1*C*, dorsomorphin markedly reduces ACC phosphorylation, although, consistent with other reports, some AMPK activity appears to remain, even at high drug concentrations (23). Therefore, we selected 5 μM as the lowest dose at which maximal inhibition of ACC phosphorylation occurs. As shown in Fig. 1*D*, 5 μM dorsomorphin markedly reduces lysosomal V-ATPase activity and blocks the increase upon amino acid starvation, suggesting

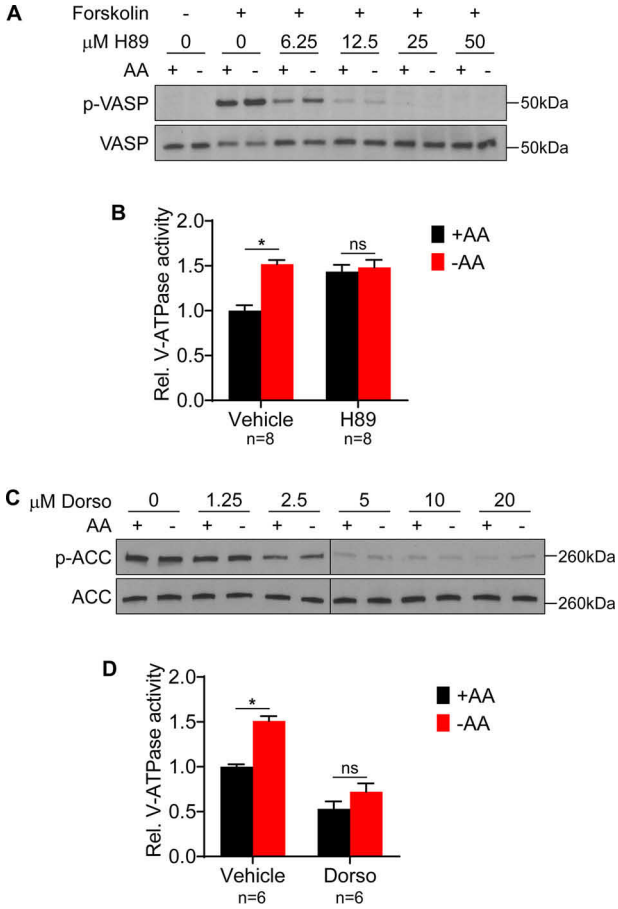

Figure 1. PKA and AMPK inhibitors modulate lysosomal V-ATPase activity in the presence and absence of amino acids. *A*, HEK293T cells were incubated for 1 h with DMSO (vehicle) or 50 μM forskolin in the presence of increasing concentrations of the PKA inhibitor H89. Lysates were prepared and subjected to Western blotting with the indicated antibodies as described in *Experimental procedures*. Representative images are shown (n = 3). *B*, HEK293T cells were incubated with FITC-dextran to allow endocytic uptake into lysosomes and then treated for 1 h with DMSO (vehicle) or 50 μM H89 in the presence (+AA) or absence (−AA) of amino acids. The rate of V-ATPase–dependent fluorescence quenching in lysosomes was determined as described in *Experimental procedures*. Values are expressed relative to the unstarved, vehicle-treated condition. *, $p < 0.05$; ns, $p \geq 0.05$. Error bars represent S.E. *C*, HEK293T cells were treated with either DMSO (vehicle) or increasing concentrations of the AMPK inhibitor dorsomorphin. Lysates were subjected to Western blotting with the indicated antibodies. Representative images are shown (n = 2). *D*, The rate of V-ATPase–dependent fluorescence quenching in FITC-dextran-loaded lysosomes was determined for HEK293T cells treated for 1 h with either DMSO (vehicle) or 5 μM dorsomorphin in the presence (+AA) or absence (−AA) of amino acids. Values are expressed relative to the unstarved, vehicle-treated condition. *, $p < 0.05$; ns, $p \geq 0.05$. Error bars represent S.E.

AMPK is important both for maintaining basal V-ATPase activity and for increasing activity during starvation.

PKA and AMPK are not required to increase lysosomal V-ATPase activity in response to amino acid starvation

H89 and dorsomorphin were found to modulate lysosomal V-ATPase activity in the presence and absence of amino acids, suggesting PKA and AMPK regulate V-ATPase activity both under basal conditions and in response to starvation. However, because these compounds are known to have numerous off-target effects (23, 24), we wished to confirm these results with genetic disruption of PKA and AMPK. We chose to

functionally disrupt PKA and AMPK by targeting the genes encoding their respective catalytic subunits using CRISPR-mediated genome editing. The PKA catalytic subunit has two main isoforms: PKA Cα, encoded by *PRKACA*, and PKA Cβ, encoded by *PRKACB* (25). To disrupt PKA, we first transfected HEK293T cells with a plasmid containing the Cas9 nuclease, an enhanced GFP reporter, and guide sequences targeting *PRKACA*. Individual GFP-positive cells were sorted by FACS, and clonal populations were expanded. Multiple clones were derived and tested for knockout of PKA Cα by Western blotting. A successful PKA Cα knockout clone then was subjected to a second round of CRISPR to knock out PKA Cβ. Successful deletion of both PKA Cα and Cβ was confirmed in multiple clones by Western blotting (Fig. 2*A*). PKA function was then probed by stimulating cells with the PKA activator forskolin, and PKA activity was monitored by phosphorylation of VASP. As shown in Fig. 2*B*, PKA Cα/Cβ double knockout cells have nearly undetectable levels of phospho-VASP, even after forskolin stimulation. We next tested the ability of PKA Cα/Cβ double knockout cells to show increased V-ATPase activity upon amino acid starvation. Surprisingly, the PKA Cα/Cβ double knockout clones are unaffected in their ability to show increased lysosomal V-ATPase activity upon amino acid starvation (Fig. 2*C*), suggesting that PKA is not required for this effect. Furthermore, PKA Cα/Cβ double knockout clones do not exhibit a significantly different level of basal lysosomal V-ATPase activity compared with WT HEK293T cells (Fig. 2*D*). This suggests that PKA does not function to suppress lysosomal V-ATPase activity under basal conditions. Finally, H89 increased lysosomal V-ATPase activity in a PKA Cα/Cβ double knockout clone, further indicating that H89 modulates V-ATPase activity independently of its effect as a PKA inhibitor (Fig. 2*E*).

We used a similar double knockout approach to disrupt AMPK. The AMPK catalytic subunit has two isoforms: AMPKα1, encoded by *PRKAA1*, and AMPKα2, encoded by *PRKAA2* (26). We confirmed knockouts by Western blotting using isoform-specific antibodies and also confirmed that phosphorylation of ACC was nearly undetectable in AMPKα1/α2 double knockout cells (Fig. 3*A*). Surprisingly, AMPKα1/α2 double knockouts are also unaffected in their ability to show increased lysosomal V-ATPase activity in response to starvation, suggesting that AMPK also is not required for this effect (Fig. 3*B*). Moreover, the AMPKα1/α2 double knockout clone did not have reduced basal lysosomal V-ATPase activity relative to that of WT cells (Fig. 3*C*). We also found that dorsomorphin reduced lysosomal V-ATPase activity in this AMPKα1/α2 double knockout clone, further indicating that dorsomorphin modulates V-ATPase activity independently of its effect as an AMPK inhibitor (Fig. 3*D*). Collectively, these results demonstrate that PKA and AMPK are not required for amino acid-dependent changes in lysosomal V-ATPase activity.

AKT1 and AKT3, but not AKT2, are involved in the increase in lysosomal V-ATPase activity upon amino acid starvation

We next tested inhibitors of other signaling pathways that have been implicated in controlling V-ATPase activity. Interestingly, while the PI3K inhibitor LY294002 does not prevent the starvation-dependent increase in V-ATPase activity (17), the AKT inhibitor MK2206 was found to block the response to starvation (Fig. 4*A*). This result suggests that AKT is important in controlling the starvation-dependent increase in V-ATPase activity despite the fact that no starvation-dependent change in AKT activity (as measured by phospho-AKT Western blotting) is observed in HEK293T cells (Fig. 4*B*). We next sought to test the function of AKT in amino acid-dependent changes in V-ATPase activity genetically. AKT triple knockout cells do not proliferate and, therefore, are not suitable for cell culture (27). However, murine lung fibroblasts have been generated that lack endogenous AKT and instead express one of each of the three individual human AKT isoforms (28), as confirmed by Western blotting using isoform-specific AKT antibodies (Fig. 4*C*). We tested the ability of these AKT knockout fibroblasts to display increased lysosomal V-ATPase activity upon amino acid starvation. Interestingly, cells expressing only AKT1 or AKT3 exhibit the same 1.5-fold increase in V-ATPase activity observed with the WT HEK293T cells upon starvation (Fig. 4*D*). In contrast, fibroblasts expressing only AKT2 show no increase in V-ATPase activity in response to amino acid starvation. These results suggest that AKT is important for controlling lysosomal V-ATPase activity in response to changes in amino acid availability, and that this dependence is specific to particular isoforms of AKT.

We next sought to further confirm our finding that particular AKT isoforms are important for controlling lysosomal V-ATPase activity in response to amino acid starvation. Because the mouse fibroblasts tested overexpress human AKT isoforms, we wished to test human cells expressing endogenous levels of AKT. Interestingly, Western blot analysis indicates that HEK293T cells express only AKT1 and AKT2 but lack AKT3 (Fig. 4*C*). Since fibroblasts expressing only AKT2 show no starvation-dependent increase in V-ATPase activity, we hypothesized that knocking out AKT1 in HEK293T cells (leaving only AKT2 intact) would block this response, whereas knocking out AKT2 (leaving only AKT1 intact) would have no effect. We targeted the *AKT1* and *AKT2* genes separately by CRISPR and confirmed, by Western blotting, the absence of the corresponding isoform in multiple independently derived clones (Fig. 5*A*). As further shown in Fig. 5*A*, there does not appear to be any substantial compensation by overexpression of other isoforms (including AKT3) in any of the derived clones.

We next tested the effect of amino acid starvation on lysosomal V-ATPase activity in the AKT knockout clones. As shown in Fig. 5*B*, AKT2 knockout cells show a normal starvation-dependent increase in lysosomal V-ATPase activity relative to WT cells. In contrast, all AKT1 knockout clones tested have a greatly diminished response of lysosomal V-ATPase activity to starvation. Four clones showed no significant increase in V-ATPase activity upon starvation, while in four other clones the increase was significantly lower than that in WT cells. Thus, the mean V-ATPase activity upon starvation relative to the unstarved condition was 1.64 ± 0.02 in WT cells, 1.64 ± 0.09 in the negative-control clones, 1.14 ± 0.07 in AKT1 knockout clones, and 1.75 ± 0.09 in AKT2 knockout clones.

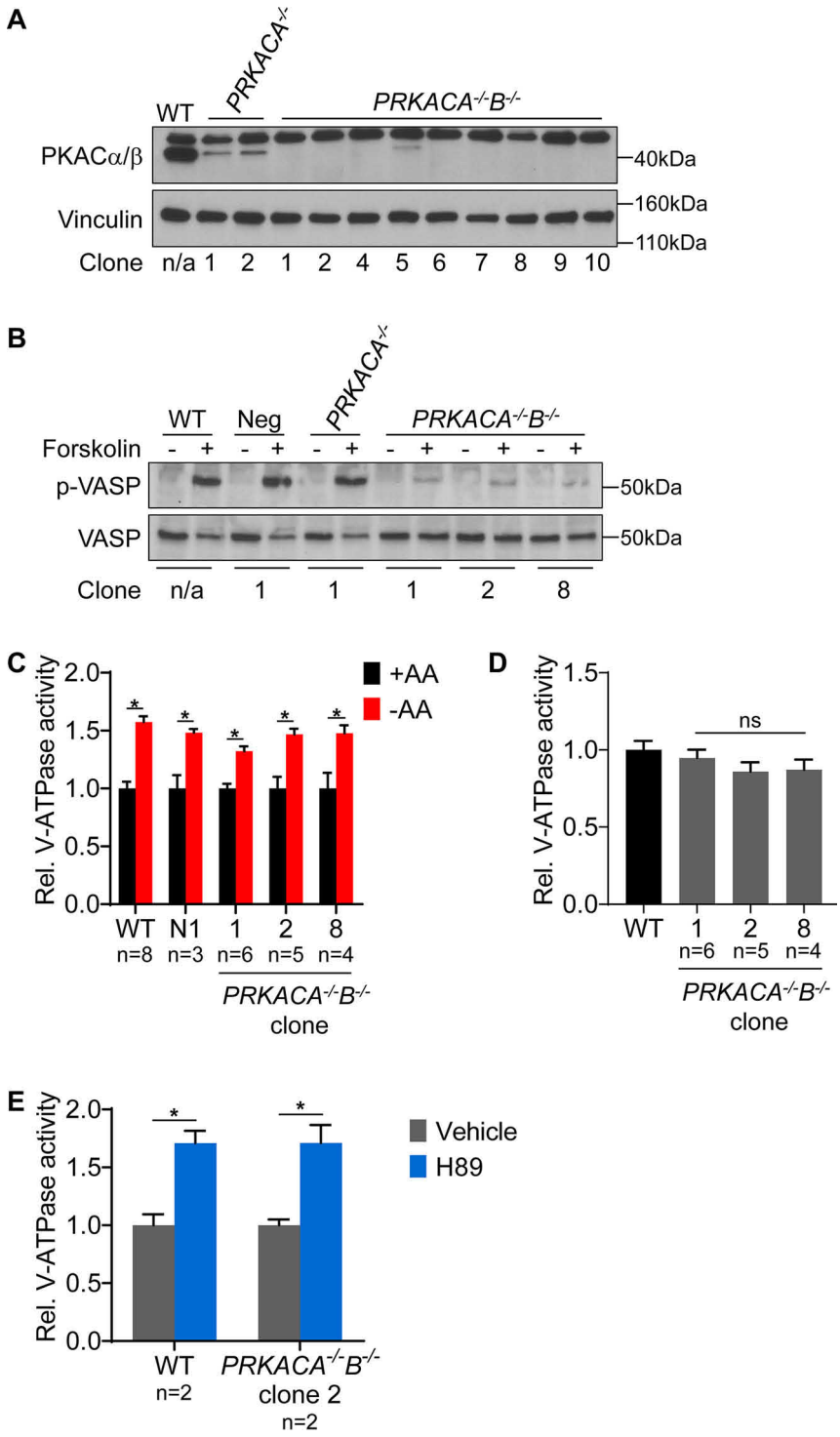

Figure 2. PKA is not required for increased lysosomal V-ATPase activity upon amino acid starvation. *A*, CRISPR-mediated genome editing was used to disrupt PKA by targeting the *PRKACA* and *PRKACB* genes as described in *Experimental procedures*. Western blotting was performed on lysates from untransfected WT cells (WT), clones targeted for disruption of PKA Cα followed by a nontargeting control (*PRKACA*$^{-/-}$), and clones targeted for disruption of PKA Cα followed by the disruption of PKA Cβ (*PRKACA*$^{-/-}$*B*$^{-/-}$). The antibody recognizes both Cα and Cβ isoforms at the correct molecular weight of 40 kDa. The antibody also produces a nonspecific band at ~50 kDa. Successful knockout results in loss of the 40-kDa band. Vinculin was used as a loading control. Representative images are shown (n = 2). *B*, To assess PKA activity, WT, nontarget negative control (Neg), PKA Cα knockout (*PRKACA*$^{-/-}$), and PKA Cα/Cβ double knockout (*PRKACA*$^{-/-}$*B*$^{-/-}$) HEK293T cells were stimulated with DMSO or 50 μM forskolin for 1 h, followed by Western blotting to detect phosphorylation of VASP. Representative images are shown (n = 2). *C*, WT, nontargeted negative control (Neg), and PKA Cα/Cβ double knockout (*PRKACA*$^{-/-}$*B*$^{-/-}$) HEK293T cells were incubated with FITC-dextran and then either maintained in amino acids (+AA) or starved (−AA) for 1 h. The rate of V-ATPase–dependent fluorescence quenching in lysosomes was determined as described previously. Values are expressed relative to the unstarved condition for each clone tested. *, $p < 0.05$; ns, $p \geq 0.05$. Error bars represent S.E. *D*, Lysosomal V-ATPase activity for unstarved PKA Cα/Cβ double knockout clones (*PRKACA*$^{-/-}$*B*$^{-/-}$) is shown relative to the unstarved WT cells. ns, $p \geq 0.05$. Error bars represent S.E. *E*, The rate of V-ATPase–dependent fluorescence quenching in FITC-dextran-loaded lysosomes was determined for WT and PKA Cα/Cβ double knockout HEK293T cells (*PRKACA*$^{-/-}$*B*$^{-/-}$) treated for 1 h with either DMSO (vehicle) or 50 μM H89 in the presence of amino acids. Values are expressed relative to the unstarved, vehicle-treated condition. *, $p < 0.05$; ns, $p \geq 0.05$. Error bars represent S.E.

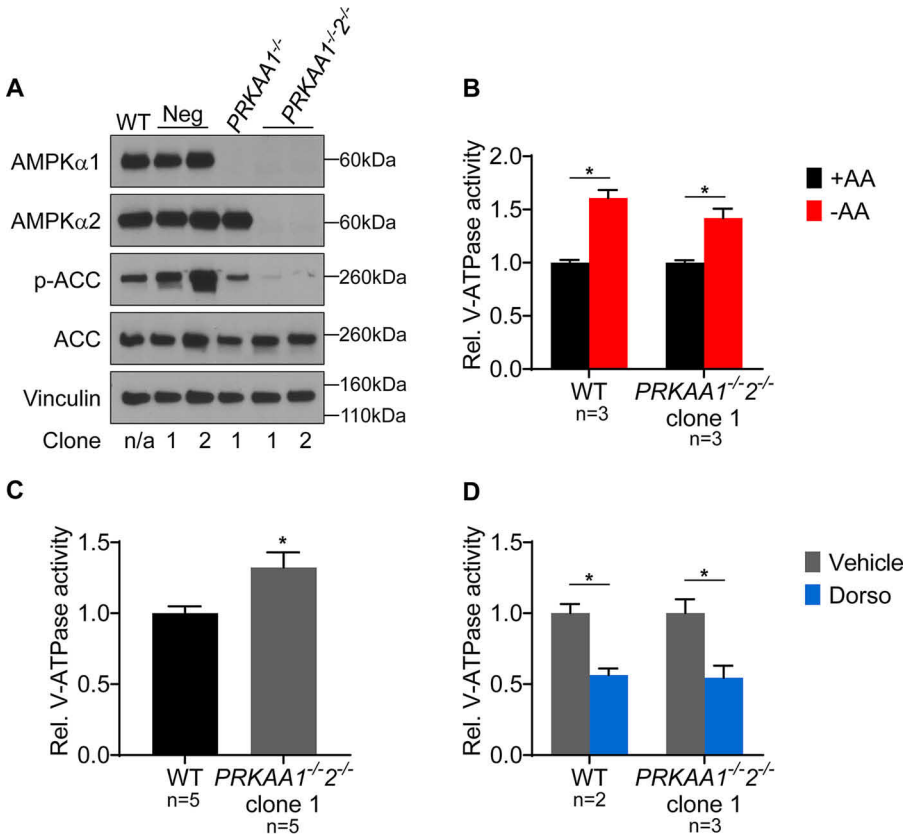

Figure 3. AMPK is not required for increased lysosomal V-ATPase activity upon amino acid starvation. *A*, CRISPR-mediated genome editing was used to disrupt AMPK by targeting the *PRKAA1* and *PRKAA2* genes as described in *Experimental procedures*. Western blotting was performed on lysates from untransfected WT cells, clones transfected with nontargeting control plasmids (Neg), clones targeted for disruption of AMPKα1 followed by nontargeting control (*PRKAA1*$^{-/-}$), and clones targeted for disruption of AMPKα1 followed by disruption of AMPKα2 (*PRKAA1*$^{-/-}$*2*$^{-/-}$). Isoform-specific AMPKα antibodies were used to assess protein knockdown, and ACC phosphorylation was used to measure AMPK activity. Vinculin was used as a loading control. Representative images are shown ($n = 2$). *B*, WT and AMPKα1/2 double knockout (*PRKAA1*$^{-/-}$*2*$^{-/-}$) HEK293T cells were loaded with FITC-dextran and then either maintained in amino acids (+AA) or starved (−AA) for 1 h. The rate of V-ATPase–dependent fluorescence quenching in lysosomes was determined as described previously. Values are expressed relative to the unstarved condition for each clone tested. *, $p < 0.05$; ns, $p \geq 0.05$. Error bars represent S.E. *C*, Lysosomal V-ATPase activity for unstarved AMPKα1/2 double knockout cells (*PRKAA1*$^{-/-}$*2*$^{-/-}$) is shown relative to unstarved WT cells. *, $p < 0.05$; ns, $p \geq 0.05$. Error bars represent S.E. *D*, The rate of V-ATPase–dependent fluorescence quenching in FITC-dextran–loaded lysosomes was determined for WT and AMPKα1/2 double knockout HEK293T cells (*PRKAA1*$^{-/-}$*2*$^{-/-}$) treated for 1 h with either DMSO (vehicle) or 5 μM dorsomorphin (Dorso) in the presence of amino acids. Values are expressed relative to the unstarved, vehicle-treated condition. *, $p < 0.05$; ns, $p \geq 0.05$. Error bars represent S.E.

Since it is possible that the lack of a starvation-dependent increase in activity is due to elevated basal activity in the AKT1 knockout cells, we also analyzed basal activity relative to WT cells. As shown in Fig. 5*C*, there is variability in basal activity among all groups, including the negative-control clones, although mean basal activities were quite similar to those of the WT. Thus, the mean basal lysosomal V-ATPase activity, relative to the WT, was 1.08 ± 0.12 in the negative control clones, 1.08 ± 0.08 in the AKT1 knockout clones, and 1.01 ± 0.09 in the AKT2 knockout clones. Importantly, among the four AKT1 knockout clones that showed no significant increase in V-ATPase activity upon starvation, no clone had a basal activity higher than 0.98 relative to the WT. Thus, for these clones, the lack of a starvation-dependent increase in lysosomal V-ATPase activity was not due to elevated basal activity.

We next wished to test whether the reduced response of lysosomal V-ATPase activity observed in the AKT1 knockout clones was due to an attenuated increase in V-ATPase assembly. To measure V-ATPase assembly, Western blotting was performed on membrane and cytosolic fractions isolated from cells that had either been maintained in amino acids or starved for 1 h. Because the peripheral V_1 domain is only present in membranes in fully assembled V-ATPase complexes, the abundance of V_1 subunits in the membrane fraction reflects the level of V-ATPase assembly (14, 17). As shown in Fig. 6, amino acid starvation led to significantly increased assembly in WT HEK293T cells and an AKT2 knockout clone, while there was no significant change in the AKT1 knockout clone.

Since it is possible that the lack of a starvation-dependent increase in assembly is due to elevated basal assembly in the AKT1 knockout cells, we also analyzed basal assembly relative to WT cells. As shown in Fig. 6*C*, the AKT1 knockout clone did have significantly increased basal assembly relative to the WT, while the AKT2 knockout clone did not. This suggests that increased basal assembly may contribute to the failure to show increased V-ATPase assembly upon amino acid starvation in this AKT1 knockout clone.

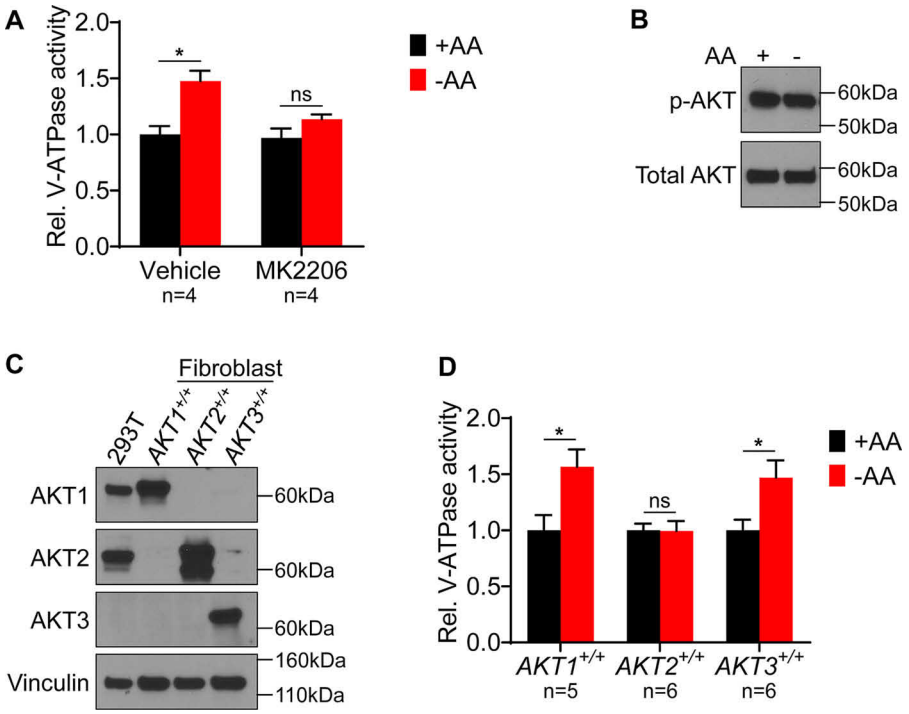

Figure 4. Effect of AKT inhibition and individual isoform expression on lysosomal V-ATPase activity and response to amino acid starvation. *A*, The rate of V-ATPase–dependent fluorescence quenching in FITC-dextran-loaded lysosomes was determined for HEK293T cells treated for 1 h with either DMSO (vehicle) or 1 μM MK2206 in the presence (+AA) or absence (−AA) of amino acids. Values are expressed relative to the unstarved, vehicle-treated condition. *, $p < 0.05$; ns, $p \geq 0.05$. Error bars represent S.E. *B*, HEK293T cells were maintained in amino acids (AA) or starved for 1 h. Lysates were prepared and subjected to Western blotting with the indicated antibodies. The phosphorylated AKT (p-AKT) antibody recognizes AKT1 phospho-S473, AKT2 phospho-S474, and AKT3 phospho-S472. The total AKT antibody recognizes AKT1, AKT2, and AKT3. Representative images are shown ($n = 2$). *C*, Western blotting was performed using isoform-specific AKT antibodies on lysates from HEK293T cells and from immortalized mouse lung fibroblasts lacking endogenous AKT and expressing individual human AKT isoforms. Representative images are shown ($n = 2$). *D*, Mouse lung fibroblasts lacking endogenous AKT and expressing individual human AKT isoforms were maintained in amino acids (+AA) or starved (−AA) for 1 h, and the rate of V-ATPase–dependent fluorescence quenching in FITC-dextran–loaded lysosomes was determined as described previously. Values are expressed relative to the unstarved condition for each cell line. *, $p < 0.05$; ns, $p \geq 0.05$. Error bars represent S.E.

These results, taken collectively with data from the AKT knockout fibroblasts and the effect of the AKT inhibitor MK2206, demonstrate that AKT is involved in the starvation-dependent increase in lysosomal V-ATPase activity and assembly, and that this involvement depends upon the isoform of AKT expressed.

Discussion

Amino acid sensing is essential to cellular homeostasis, and the V-ATPase has emerged as a central component of the amino acid sensing machinery in mammalian cells (29). The V-ATPase is required for amino acid-dependent association of mTORC1 with the lysosomal membrane, where it is activated (30, 31). Furthermore, our laboratory previously reported that amino acids modulate V-ATPase assembly and activity on lysosomes, and that this effect is PI3K- and mTORC1-independent (17). We also showed that this starvation-dependent increase in lysosomal V-ATPase activity is not required for amino acid-dependent changes in mTORC1 activity (17). Rather, the increase in lysosomal acidification observed upon amino acid starvation likely facilitates a rapid increase in lysosomal protein degradation, thereby helping to maintain amino acid homeostasis.

In the present study, we sought to identify the signaling pathways controlling lysosomal V-ATPase activity in response to changes in amino acid availability. We first investigated the roles of PKA and AMPK, because these kinases appear to be important for controlling V-ATPase assembly in response to changes in glucose levels in yeast and mammalian cells, respectively (12, 14). Treatment of cells with the PKA inhibitor H89 robustly increases lysosomal V-ATPase activity in the presence of amino acids and prevents any further increase upon amino acid starvation. It should be noted that with the concentration of H89 at which PKA is fully inhibited, V-ATPase activity is likely saturated, which may be why no further increase is observed upon starvation. This result would suggest that PKA functions to suppress lysosomal V-ATPase activity in mammalian cells. In contrast, in yeast, PKA functions to increase V-ATPase assembly and activity upon glucose starvation (12). Based upon this pharmacological result, we expected that PKA Cα/Cβ double knockout cells would have elevated lysosomal V-ATPase activity, which would be insensitive to amino acid starvation. Surprisingly, we observed that PKA Cα/Cβ double knockout cells have normal basal levels of lysosomal V-ATPase activity and display a normal increase in activity upon amino acid starvation. This suggests that PKA does not function to regulate lysosomal V-ATPase activity in mammalian cells in response to starvation, and that H89 modulates V-ATPase activity by altering the activity of other targets. H89 was originally described as a Rho-associated protein kinase (ROCK) inhibitor

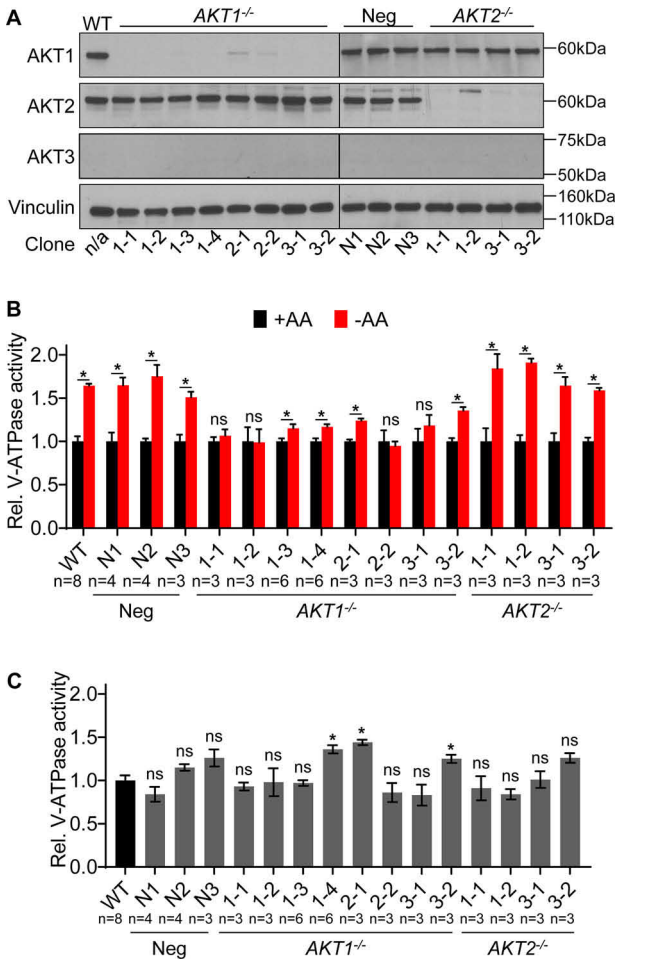

Figure 5. AKT1 knockout HEK293T cells have reduced ability to increase lysosomal V-ATPase activity in response to amino acid starvation. *A*, 3 different guide sequences were used to target either *AKT1* or *AKT2* for CRISPR-mediated disruption in HEK293T cells. Western blotting was performed on lysates from untransfected WT cells, clones transfected with non-targeting control plasmids (Neg), clones targeted for disruption of AKT1 ($AKT1^{-/-}$), and clones targeted for disruption of AKT2 ($AKT2^{-/-}$). Isoform-specific AKT antibodies were used to assess protein knockdown, and vinculin was used as a loading control. Representative images are shown ($n = 3$). *B*, WT, nontargeted negative control (Neg), AKT1 knockout ($AKT1^{-/-}$), and AKT2 knockout ($AKT2^{-/-}$) HEK293T cells were incubated with FITC-dextran and then either maintained in amino acids (+AA) or starved for 1 h (−AA). The rate of V-ATPase–dependent fluorescence quenching in lysosomes was determined as described previously. Values are expressed relative to the unstarved condition for each clone tested. AKT2 knockout cells displayed a statistically significant increase in V-ATPase activity following amino acid starvation, whereas AKT1 knockout cells did not. *, $p < 0.05$; ns, $p \geq 0.05$. Error bars represent S.E. *C*, Lysosomal V-ATPase activity for unstarved CRISPR negative control (neg), AKT1 knockout ($AKT1^{-/-}$), and AKT2 knockout ($AKT2^{-/-}$) cells is shown relative to unstarved WT cells. *, $p < 0.05$; ns, $p \geq 0.05$. Error bars represent S.E.

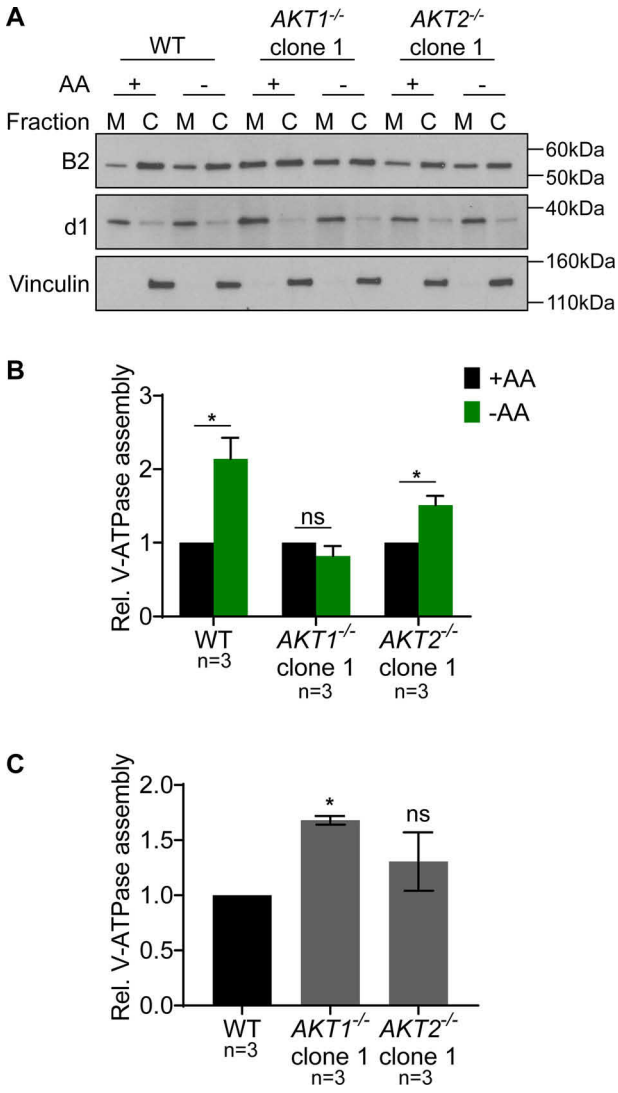

Figure 6. AKT1 knockout HEK293T cells fail to show increased V-ATPase assembly in response to amino acid starvation. *A*, WT HEK293T cells, an AKT1 knockout clone ($AKT1^{-/-}$), and an AKT2 knockout clone ($AKT2^{-/-}$) were maintained in amino acids or starved for 1 h, followed by cell fractionation, as described in *Experimental procedures*. Western blotting was performed on the membrane (M) and cytosolic (*C*) fractions using the indicated antibodies. B2 is a V_1 subunit and, therefore, indicates the abundance of the V_1 domain in each fraction. d1 is a V_0 subunit and was used as a membrane loading control, while vinculin was used as a cytosolic loading control. The relative abundance of V_1 in the membrane fraction *versus* the cytosolic fraction is a measure of V-ATPase assembly. Representative images are shown ($n = 3$). *B*, Quantification of Western blots described in panel *A*. The intensity of B2 in the membrane fraction was normalized to d1. The intensity of B2 in the cytosolic fraction was normalized to vinculin. The ratio of the normalized intensities gives the relative assembly. Values are expressed relative to the unstarved condition for each clone tested. WT and AKT2 knockout ($AKT2^{-/-}$) cells displayed a statistically significant increase in V-ATPase assembly following amino acid starvation, whereas AKT1 knockout ($AKT1^{-/-}$) cells did not. *, $p < 0.05$; ns, $p \geq 0.05$. Error bars represent S.E. *C*, V-ATPase assembly for an unstarved AKT1 knockout clone ($AKT1^{-/-}$) and an unstarved AKT2 knockout clone ($AKT2^{-/-}$) is shown relative to unstarved WT cells. *, $p < 0.05$; ns, $p \geq 0.05$. Error bars represent S.E.

and is now known to potently inhibit numerous other kinases as well (24). H89 was reported to induce autophagy in a PKA-independent manner, and this effect was partially abrogated by the inhibition of AKT (32). While lysosomal acidification was not measured in that study, it is tempting to speculate that the increased lysosomal V-ATPase activity we observed upon H89 treatment is related to the increased autophagic flux that these authors observed. Further studies will be necessary to elucidate the mechanism by which H89 increases lysosomal V-ATPase activity.

In contrast to H89, which increases lysosomal V-ATPase activity, we found that the treatment of HEK293T cells with the AMPK inhibitor dorsomorphin significantly lowers lysosomal V-ATPase activity and also prevents any increase upon amino acid starvation. Dorsomorphin was originally discovered as an

AMPK inhibitor but is now known to inhibit numerous kinases more potently than AMPK, making interpretation of results obtained with this compound challenging (23, 24). Using CRISPR-mediated gene disruption, we found that AMPKα1/α2 double knockout cells display normal levels of lysosomal V-ATPase activity and also show increased activity upon amino acid starvation. This suggests that in mammalian cells, AMPK is not required to maintain lysosomal V-ATPase activity and does not control the response to amino acid starvation. Recent studies have reported that AMPK is activated at the lysosome in a V-ATPase–dependent manner during energy stress (33). Therefore, while AMPK may not be required for changes to lysosomal V-ATPase activity upon amino acid starvation, it may be important during other forms of nutrient depletion, such as glucose starvation (14).

We previously showed that the treatment of cells with the PI3K catalytic inhibitor LY294002 does not prevent starvation-induced increases in V-ATPase assembly and activity (17). In response to external stimuli, such as growth factors and insulin, PI3K converts plasma membrane PI(4,5)P_2 to PI(3,4,5)P_3, which recruits AKT for activation. Therefore, it was surprising that cells treated with the AKT allosteric inhibitor MK2206 do not show a starvation-dependent increase in lysosomal V-ATPase activity. It was further surprising that AKT activation (measured by Western blotting for AKT phospho-S473) does not increase upon amino acid starvation. These findings suggest that the existing pool of active AKT is sufficient to control the response of V-ATPase to amino acid starvation. Thus, LY294002 prevents any further AKT activation, but active AKT molecules may still be able to regulate downstream substrates until they are deactivated by phosphatases. Conversely, MK2206 directly inhibits all cellular AKT, which could explain the different responses to the two drugs.

A major downstream effector of AKT is mTORC1, which is activated at the lysosome following amino acid-dependent recruitment by a complex containing the V-ATPase (31). We previously showed that the starvation-dependent increases in V-ATPase activity and assembly still occur in the presence of mTORC1 inhibition with rapamycin (17). The fact that mTORC1 is not required for the increased V-ATPase activity upon amino acid starvation raises mechanistic questions of how AKT controls V-ATPase activity. AKT has been reported to directly bind the V-ATPase to increase endosomal acidification during rotavirus infection (34). This presents the possibility that AKT binding to the V-ATPase is a conserved mechanism to control activity in mammalian cells. Alternatively, AKT may act on intermediate proteins, such as assembly factors, to regulate lysosomal V-ATPase activity. Whether acting on the V-ATPase directly or indirectly, AKT may translocate to lysosomes to regulate lysosomal V-ATPase activity and/or assembly. There is a growing body of evidence to support a role for the intracellular translocation of AKT. Starvation of cells was shown to lead to lysosomal recruitment of AKT by pleckstrin homology domain-containing family F member 2 (Phafin2) and the serine/threonine kinase VRK2 (35, 36). Moreover, lysosomal recruitment of AKT appears to be important for lysosomal acidification and autophagic flux (35). Although those studies were done with a more prolonged and complete starvation than was performed in the present study, they nevertheless provide further evidence in support of a role for AKT in regulating lysosomal acidification during nutrient limitation.

We have begun to investigate the role of AKT isoforms in controlling lysosomal V-ATPase activity in response to amino acid availability. AKT exists as three highly homologous isoforms, encoded by the genes *AKT1*, *AKT2*, and *AKT3*. While largely redundant in their activation and downstream substrates, genetic studies have revealed AKT isoform-specific phenotypes (18). Because AKT triple knockout cells are not viable for long-term culture, we first took advantage of mouse fibroblast lines, which express only one of the three human AKT isoforms and in which the endogenous mouse AKT has been disrupted (28). We found that cells expressing only AKT1 or only AKT3 display increased lysosomal V-ATPase activity upon amino acid starvation, whereas cells expressing only AKT2 show no change upon starvation. This result provides additional evidence for a role of AKT in the regulation of lysosomal V-ATPase activity and suggests that particular AKT isoforms are important for this process. Since we find HEK293T cells have no detectible AKT3 expression, we hypothesized that knocking out AKT1 (leaving AKT2 intact) would abrogate the increased V-ATPase activity upon amino acid starvation. Indeed, CRISPR-mediated AKT1 knockouts display a significantly reduced response to amino acid starvation. Although some starvation-dependent increase in activity is still observed in some clones, it is possible that these cells still express low levels of AKT1, or that other mechanisms exist that can compensate for AKT1 loss under certain circumstances.

Assembly is a major form of V-ATPase regulation, and we previously showed that amino acid starvation leads to a significant increase in V-ATPase assembly in mammalian cells (17). Other V-ATPase–dependent mechanisms that can influence lysosomal acidification include changes to the coupling efficiency of the enzyme and changes in the density of V-ATPase complexes per lysosome (1, 4). Therefore, it was important to test whether the reduced response to amino acid starvation in the AKT1 knockouts is due to a failure to increase V-ATPase assembly. We find that while WT and AKT2 knockout cells display a significant increase in V-ATPase assembly upon amino acid starvation, AKT1 knockout cells show no significant change. However, the failure to show increased assembly upon starvation may be because this AKT1 knockout clone displays significantly elevated basal V-ATPase assembly. This clone does not have elevated basal lysosomal V-ATPase activity, suggesting that the assembled lysosomal V-ATPases are not active. Alternatively, since assembly was measured in whole-cell lysates, whereas activity is measured in lysosomes, it is possible that the observed basal elevation is due to the assembly of V-ATPase complexes in other cell membranes. However, studies using several different types of mammalian cells have reported that the V_0 domain (and, thus, assembly-competent V-ATPase) is most abundant in lysosomal fractions (37–39). Furthermore, we have previously found that changes in lysosomal V-ATPase activity strongly correlate with changes in total cellular V-ATPase assembly in HEK293T cells (14, 17). Therefore, it is likely that the lysosomal pool of V-ATPases contributes to a significant fraction of the observed change in total cellular V-ATPase assembly.

In summary, we have shown that AKT plays an important role in modulating V-ATPase–dependent lysosomal acidification in response to amino acid starvation. Future studies will investigate the mechanism by which AKT regulates V-ATPase assembly and activity in response to nutrient stress and test the hypothesis that this response is a primitive mechanism to rapidly increase protein degradation upon starvation to replenish the supply of free amino acids. Understanding how cells sense and respond to amino acid availability may enable the development of treatments for conditions in which nutrient homeostasis is dysregulated, such as cancer and diabetes. In addition, understanding how lysosomal acidification is controlled may lead to the development of therapies for lysosomal storage and neurodegenerative diseases, such as Alzheimer's disease, which are characterized by the failure to degrade toxic protein aggregates.

Experimental procedures

Cell culture

HEK293T cells were obtained from ATCC (CRL-3216), and AKT knockout mouse lung fibroblasts were a gift from Dr. Philip Hinds (Tufts University). WT, CRISPR negative-control, PKA Cα/Cβ double knockout, and AKT knockout HEK293T cells were grown in minimum essential medium (MEM) (no. 11095; Gibco) supplemented with 10% FBS (no. 12306C; Sigma-Aldrich) and 1% penicillin-streptomycin (pen/strep; no. 15140; Gibco). AMPKα1/α2 double knockout HEK293T cells were grown in DMEM (no. 11995; Gibco) supplemented with 10% FBS and 1% pen/strep. AKT knockout mouse lung fibroblasts were grown in DMEM supplemented with 10% FBS, 1% MEM nonessential amino acids (no. 11995; Gibco), 0.5% GlutaMAX (no. 35050; Gibco), and 1% pen/strep. All cells were grown on tissue culture-treated polystyrene dishes and routinely passaged by detaching with 0.05% Trypsin-EDTA (no. 25300; Gibco). Cells were maintained in a humidified environment at 37 °C with 5% CO_2. Cells were discarded after reaching passage 15.

Amino acid starvation media

A 10× stock solution of amino acids was prepared by dissolving individual powdered amino acids in PBS (no. 10010; Gibco), filter sterilized, and stored as aliquots at −20 °C. The final (1×) amino acid concentrations were the following: 0.05 mM L-alanine, 0.7 mM L-arginine hydrochloride, 0.05 mM L-asparagine, 0.05 mM L-aspartic acid, 0.2 mM L-cysteine, 0.05 mM L-glutamic acid monosodium salt, 2.5 mM L-glutamine, 0.25 mM glycine, 0.15 mM L-histidine hydrochloride monohydrate, 0.42 mM L-isoleucine, 0.45 mM L-leucine, 0.5 mM L-lysine hydrochloride, 0.12 mM L-methionine, 0.21 mM L-phenylalanine, 0.15 mM L-proline, 0.25 mM L-serine, 0.45 mM L-threonine, 0.04 mM L-tryptophan, 0.21 mM L-tyrosine, and 0.45 mM L-valine. All amino acids were purchased from Sigma-Aldrich. DMEM/F12 without amino acids (no. D9811-01; US Biological) was prepared in ultrapure water, brought to pH 7.2, and filter sterilized. Prepared amino acid-free medium was discarded after 1 month. The 10× amino acid solution (or an equivalent volume of PBS) was added to amino acid-free medium immediately before each starvation experiment, for a final concentration of 1×.

V-ATPase–dependent lysosomal proton pumping

2×10^6 cells were seeded onto 6-cm cell culture dishes that had been coated with 0.1 mg/ml poly-D-lysine (PDL; no. A-003-E; Millipore) and allowed to attach overnight. The following day, the growth medium was replaced with medium containing 2 mg/ml FITC-dextran (average molecular weight, 40 kDa; no. FD40; Sigma-Aldrich), and the cells were incubated overnight to allow the uptake of the dextran by fluid-phase endocytosis. The next day, the cell monolayers were rinsed with warm PBS and incubated with fresh medium without FITC-dextran for 1 h to chase the internalized FITC-dextran to lysosomes. Following the chase period, cell monolayers were rinsed with warm PBS and then incubated for 1 h with starvation medium containing 1× amino acids or PBS in the presence or absence of the indicated inhibitors. Following the 1 h treatment period, cell monolayers were rinsed with ice-cold PBS and scraped into 200 μl ice-cold activity assay buffer (125 mM KCl, 50 mM sucrose, 20 mM HEPES, pH 7.5, 1 mM EDTA, 1 mM PMSF, 5 μg/ml leupeptin, 2 μg/ml aprotinin, 1 μg/ml pepstatin). The cell suspensions were centrifuged at 300 × *g* for 5 min at 4 °C, and the resulting pellets were resuspended in 400 μl fresh ice-cold activity assay buffer. Cells were lysed by passing through a 27-gauge needle 20 times, and the crude lysates then were cleared of unbroken cells and nuclei by centrifugation at 1,000 × *g* for 10 min at 4 °C. The cleared supernatants then were centrifuged at 16,100 × *g* for 15 min at 4 °C to sediment FITC-dextran–containing lysosomes. The resulting pellets were resuspended in 100 μl activity assay buffer.

To measure V-ATPase–dependent lysosomal proton pumping, ~10–20 μl of sample was added to a quartz cuvette (101-058-40-QS; Hellma Analytics) containing activity assay buffer prewarmed to 37 °C. Samples were excited at 490 nm, and fluorescence emission was continuously collected at 520 nm using a Perkin-Elmer LS50B luminescence spectrophotometer. V-ATPase–dependent proton pumping was initiated by adding magnesium-ATP to a final concentration of 1 mM ATP and 2 mM Mg^{2+}. The rate of fluorescence quenching was determined by linear regression using GraphPad Prism 8.0, and the first 10 s of quenching were used for statistical analysis.

Cell fractionation

5×10^6 cells were seeded onto 10-cm, PDL-coated culture dishes and allowed to attach overnight. The next day, cell monolayers were rinsed with warm PBS and then incubated for 1 h with starvation medium containing 1× amino acids or PBS. Following the 1 h treatment period, cell monolayers were rinsed with ice-cold PBS and scraped into 500 μl ice-cold fractionation buffer (250 mM sucrose, 10 mM HEPES, pH 7.2, 1 mM EDTA, 1 mM PMSF, 5 μg/ml leupeptin, 2 μg/ml aprotinin, 1 μg/ml pepstatin, 2 mM β-glycerophosphate, 1 mM NaF). The cell suspensions were centrifuged at 300 × *g* for 5 min at 4 °C, and the resulting pellets were resuspended in 500 μl fresh ice-cold fractionation buffer. Cells were lysed by passing through a 27-gauge needle 20 times, and the crude lysates then were cleared of unbroken cells and nuclei by centrifugation at 1,000 × *g* for 10 min at 4 °C. The cleared supernatants then were centrifuged at 100,000 × *g* for 30 min at 4 °C using a Beckman Coulter L7-55

ultracentrifuge to sediment the membrane fractions. The resulting supernatants containing the cytosolic fractions were concentrated using Amicon Ultra 10K centrifugal filter units (UFC501096; Millipore) according to the manufacturer's instructions. The membrane pellets were solubilized in fractionation buffer supplemented with 1% SDS.

Western blotting

Cells were seeded onto PDL-coated culture dishes at $1 \times 10^5/cm^2$ and allowed to attach overnight. Following treatment, whole-cell lysates were prepared by rinsing cell monolayers in ice-cold PBS and scraping cells into ice-cold lysis buffer (150 mM NaCl, 50 mM Tris, pH 8, 1% Triton X-100, 2 mM β-glycerophosphate, 1 mM NaF, 1 mM PSMF, 5 μg/ml leupeptin, 2 μg/ml aprotinin, 1 μg/ml pepstatin). Lysates were rotated for 30 min at 4 °C and then centrifuged at 16,100 × *g* for 20 min at 4 °C. The protein concentrations of the resulting supernatants were determined by the Lowry method. Samples were mixed with 4× Laemmli buffer (400 mM DTT, 200 mM Tris, pH 6.8, 40% glycerol, 8% SDS, 0.05% bromphenol blue) and heated to 70 °C for 10 min. 20 μg of protein per sample was resolved on 4–15% polyacrylamide gels (no. 4561086; Bio-Rad) at 200 V for 40 min using a Bio-Rad Mini Protean III cell containing 500 ml running buffer (192 mM glycine, 25 mM Tris, 0.1% SDS). Proteins were electroblotted to nitrocellulose membranes (no. 1620115; Bio-Rad) at 100 V for 1 h in transfer buffer (200 mM glycine, 25 mM Tris, 20% methanol). Membranes were incubated in blocking buffer containing 1.5% nonfat milk in TBS-T (Tris-buffered saline with 0.1% Tween-20) for 30 min. Membranes were then incubated with primary antibodies diluted in blocking buffer (dilutions listed below) overnight at 4 °C. The following day, membranes were washed in TBS-T and then incubated for 1 h with horseradish peroxidase-conjugated anti-mouse (no. 170-6516; Bio-Rad) or anti-rabbit (no. ab97051; Abcam) secondary antibody diluted in blocking buffer at 1:3000. Membranes then were washed in TBS-T, incubated with Amersham Biosciences ECL chemiluminescent substrate (no. RPN2106; GE Healthcare), and developed on HyBlot CL autoradiography film (no. E3012; Denville Scientific).

The following primary antibodies were purchased from Cell Signaling Technology: anti-VASP (no. 3112; 1:1000), anti-phospho-ACC (Ser79) (no. 3661; 1:2000), anti-ACC (no. 3662; 1:500), anti-PKA Cα (no. 5842; 1:1000), anti-AMPKα1 (no. 2795; 1:1000), anti-AMPKα2 (no. 2757; 1:1000), anti-phospho-AKT (Ser473) (no. 4060; 1:2000), anti-AKT (pan) (no. 4691; 1:1000), anti-AKT1 (no. 2938; 1:1000), anti-AKT2 (no. 3063; 1:1000), and anti-AKT3 (no. 3788; 1:1000). The following antibodies were purchased from Abcam: anti-phospo-VASP (Ser179) (no. ab47268; 1:500), anti-PKA Cβ (detects both Cα and Cβ) (no. ab187515; 1:1000), and anti-V_0d1 (no. ab56441; 1:500). Anti-V_1B2 was purchased from Bio-Rad (no. VMA00190; 1:2000). Anti-vinculin was purchased from Sigma-Aldrich (no. V9131; 1:50,000). The molecular weights of proteins detected by Western blotting were determined by comparing their mobility to that of the Novex Sharp prestained protein standard (no. LC5800; Invitrogen).

For fractionation experiments, band intensities were quantified using ImageJ 1.52p. The intensity of subunit B2 in the cytosolic fraction of each sample was normalized to the intensity of the corresponding cytosolic loading control, vinculin. The intensity of subunit B2 in the membrane fraction was normalized to the intensity of the corresponding membrane loading control, subunit d1. V-ATPase assembly was determined by taking the ratio of normalized intensities of B2 in the membrane and cytosolic fractions.

CRISPR-mediated disruption of AMPK

The strategy to disrupt AMPK was to target first the α1 isoform of the catalytic subunit, encoded by *PRKAA1*, and then the α2 isoform, encoded by *PRKAA2*. The first exon of *PRKAA1* was searched using the online tool at crispr.mit.edu. The guide sequence GAAGATCGGCCACTACATTC was chosen because of its high specificity score and cloned into the plasmid pSpCas9(BB)-2A-Puro (PX459; no. 48139; Addgene) according to the method of Ran *et al.* (40). Plasmids containing either the guide sequence or empty backbone were transfected into HEK293T cells using Lipofectamine 2000 (no. 11668; Invitrogen) according to the manufacturer's instructions. Successfully transfected cells were selected for growth in 1 μg/ml puromycin and then seeded at 0.5 cells/well into 96-well plates by serial dilution to isolate individual clones. Clonal lines were expanded until there were enough cells to determine protein expression of AMPKα1 by Western blotting. A single AMPKα1 knockout clone was chosen for a second round of CRISPR to target *PRKAA2*, this time by cloning a published guide sequence, GAAGATCGGACACTACGTGC (41), into pSpCas9(BB)-2A-GFP (PX458; no. 48138; Addgene) according to the method of Ran *et al.* (40). Plasmids containing either the guide sequence or empty backbone were transfected into cells using Lipofectamine 3000 (no. L3000; Invitrogen) according to the manufacturer's instructions. The following day, cells were detached by trypsinization, and GFP-positive cells were sorted individually into the wells of 96-well plates by FACS. Clonal lines were subsequently expanded until there were enough cells to determine protein expression of AMPKα2 by Western blotting.

CRISPR-mediated disruption of PKA and AKT

The protein-coding regions of the *PRKACA*, *PRKACB*, *AKT1*, and *AKT2* genes were searched using the online tool CHOPCHOP (42), which scores potential single guide RNAs according to multiple parameters, including specificity, cleavage efficiency, and the likelihood of causing a frameshift. The following guide sequences were chosen to target *PRKACA*: ACGAATCAAGACCCTCGGCA, TCGTTCAAACTGATCCAAGT, and TGAACCTTCCGATCCGCCGT. The following guide sequences were chosen to target *PRKACB*: GCTGCATAGAACCGTGCATG and GCTACAATAAGGCAGTGGAT. The following guide sequences were chosen to target *AKT1*: GAGCGACGTGGCTATTGTGA, TCACGTTGGTCCACATCCTG, and GACAACCGCCATCCAGACTG. The following guide sequences were chosen to target *AKT2*: TCTCGTCTGGAGAATCCACG, GAGCCACACTTGTAGTCCAT, and GAGATAGTCGAAGTCATTCA. Plasmids containing either guide sequences or the empty backbone were transfected

into HEK293T cells using Lipofectamine 3000. The following day, cells were detached by trypsinization, and GFP-positive cells were sorted individually into the wells of 96-well plates by FACS. Clonal lines were subsequently expanded until there were enough cells to determine protein expression by Western blotting. For PKA, a single PKA Cα knockout clone was selected for a second round of CRISPR to disrupt PKA Cβ.

Other materials

The following compounds were purchased from Selleck Chemicals: H89 2HCl (no. S1582), MK2206 2HCl (no. S1078), and forskolin (no. S2449). Dorsomorphin was purchased from Sigma-Aldrich (no. P5499).

Statistics

p values were calculated using a two-tailed Student's *t* test.

Data availability

All data are available upon request to the corresponding author, Dr. Michael Forgac.

Acknowledgments—We thank Christina McGuire for many helpful discussions.

Author contributions—M. P. C., L. A. S., and M. F. conceptualization; M. P. C. and L. A. S. investigation; M. P. C. and L. A. S. methodology; M. P. C. writing-original draft; M. P. C., L. A. S., and M. F. writing-review and editing; M. F. resources; M. F. supervision; M. F. funding acquisition; M. F. project administration.

Funding and additional information—Funding was provided by Tufts Collaborative Cancer Biology Awards to M. P. C. and L. A. S., as well as National Institutes of Health Grants CA189321 to L. A. S. and GM34478 to M. F. The content is solely the responsibility of the authors and does not necessarily represent the official views of the National Institutes of Health.

Conflict of interest—The authors declare that they have no conflicts of interest with the contents of this article.

Abbreviations—The abbreviations used are: V-ATPase, vacuolar H1-ATPase; ACC, acetyl-CoA carboxylase; AKT, serine/threonine-protein kinase, also known as RAC and PKB; AMPK, 5′-AMP-activated protein kinase; AMPKα1/2, AMPK catalytic subunit alpha-1/2; DMEM, Dulbecco's modified Eagle medium; DMEM/F12, DMEM–Ham's F-12 nutrient mixture (1:1); MEM, minimum essential medium; mTORC1, mTOR complex 1; PDL, poly-d-lysine; PKA, cAMP-dependent protein kinase; PKA Cα/β, PKA catalytic subunit alpha/beta; PI3K, type I phosphoinositide 3-kinase; pen/strep, penicillin-streptomycin; VASP, vasodilator-stimulated phosphoprotein.

References

1. Forgac, M. (2007) Vacuolar ATPases: rotary proton pumps in physiology and pathophysiology. *Nat. Rev. Mol. Cell Biol.* **8,** 917–929 CrossRef Medline
2. Kane, P. M. (2007) The long physiological reach of the yeast vacuolar H+-ATPase. *J. Bioenerg. Biomembr.* **39,** 415–421 CrossRef Medline
3. Breton, S., and Brown, D. (2013) Regulation of luminal acidification by the V-ATPase. *Physiology* **28,** 318–329 CrossRef
4. Cotter, K., Stransky, L., McGuire, C., and Forgac, M. (2015) Recent insights into the structure, regulation, and function of the V-ATPases. *Trends Biochem. Sci.* **40,** 611–622 CrossRef Medline
5. Maxfield, F. R., and McGraw, T. E. (2004) Endocytic recycling. *Nat. Rev. Mol. Cell Biol.* **5,** 121–132 CrossRef Medline
6. Ghosh, P., Dahms, N. M., and Kornfeld, S. (2003) Mannose 6-phosphate receptors: new twists in the tale. *Nat. Rev. Mol. Cell Biol.* **4,** 202–212 CrossRef
7. Gu, F., and Gruenberg, J. (2000) ARF1 regulates pH-dependent COP functions in the early endocytic pathway. *J. Biol. Chem.* **275,** 8154–8160 CrossRef Medline
8. Kawai, A., Uchiyama, H., Takano, S., Nakamura, N., and Ohkuma, S. (2007) Autophagosome-lysosome fusion depends on the pH in acidic compartments in CHO cells. *Autophagy* **3,** 154–157 CrossRef Medline
9. Xu, H., and Ren, D. (2015) Lysosomal physiology. *Annu. Rev. Physiol.* **77,** 57–80 CrossRef Medline
10. Kane, P. M. (2012) Targeting reversible disassembly as a mechanism of controlling V-ATPase activity. *Curr. Protein Pept. Sci.* **13,** 117–123 CrossRef Medline
11. Parra, K. J., Chan, C.-Y., and Chen, J. (2014) Saccharomyces cerevisiae vacuolar H+-ATPase regulation by disassembly and reassembly: one structure and multiple signals. *Eukaryot. Cell* **13,** 706–714 CrossRef Medline
12. Bond, S., and Forgac, M. (2008) The Ras/cAMP/protein kinase A pathway regulates glucose-dependent assembly of the vacuolar (H+)-ATPase in yeast. *J. Biol. Chem.* **283,** 36513–36521 CrossRef Medline
13. Sautin, Y. Y., Lu, M., Gaugler, A., Zhang, L., and Gluck, S. L. (2005) Phosphatidylinositol 3-kinase-mediated effects of glucose on vacuolar H+-ATPase assembly, translocation, and acidification of intracellular compartments in renal epithelial cells. *Mol. Cell. Biol.* **25,** 575–589 CrossRef Medline
14. McGuire, C. M., and Forgac, M. (2018) Glucose starvation increases V-ATPase assembly and activity in mammalian cells through AMP kinase and phosphatidylinositide 3-kinase/Akt signaling. *J. Biol. Chem.* **293,** 9113–9123 CrossRef Medline
15. Marjuki, H., Gornitzky, A., Marathe, B. M., Ilyushina, N. A., Aldridge, J. R., Desai, G., Webby, R. J., and Webster, R. G. (2011) Influenza A virus-induced early activation of ERK and PI3K mediates V-ATPase-dependent intracellular pH change required for fusion. *Cell. Microbiol.* **13,** 587–601 CrossRef Medline
16. Liberman, R., Bond, S., Shainheit, M. G., Stadecker, M. J., and Forgac, M. (2014) Regulated assembly of vacuolar ATPase is increased during cluster disruption-induced maturation of dendritic cells through a phosphatidylinositol 3-kinase/mTOR-dependent pathway. *J. Biol. Chem.* **289,** 1355–1363 CrossRef Medline
17. Stransky, L. A., and Forgac, M. (2015) Amino Acid Availability Modulates Vacuolar H+-ATPase Assembly. *J. Biol. Chem.* **290,** 27360–27369 CrossRef Medline
18. Manning, B. D., and Toker, A. (2017) AKT/PKB Signaling: Navigating the Network. *Cell* **169,** 381–405 CrossRef Medline
19. Rein, J., Voss, M., Blenau, W., Walz, B., and Baumann, O. (2008) Hormone-induced assembly and activation of V-ATPase in blowfly salivary glands is mediated by protein kinase A. *Am. J. Physiol. Cell Physiol.* **294,** C56–C65 CrossRef
20. Hallows, K. R., Alzamora, R., Li, H., Gong, F., Smolak, C., Neumann, D., and Pastor-Soler, N. M. (2009) AMP-activated protein kinase inhibits alkaline pH- and PKA-induced apical vacuolar H+-ATPase accumulation in epididymal clear cells. *Am. J. Physiol. Cell Physiol.* **296,** C672–C681 CrossRef Medline
21. Horstrup, K., Jablonka, B., Hönig-Liedl, P., Just, M., Kochsiek, K., and Walter, U. (1994) Phosphorylation of focal adhesion vasodilator-stimulated phosphoprotein at Ser157 in intact human platelets correlates with fibrinogen receptor inhibition. *Eur. J. Biochem.* **225,** 21–27 CrossRef

22. Ha, J., Daniel, S., Broyles, S. S., and Kim, K. H. (1996) Critical phosphorylation sites for acetyl-CoA carboxylase activity. *J. Biol. Chem.* **271,** 1385–22168 CrossRef Medline
23. Vogt, J., Traynor, R., and Sapkota, G. P. (2011) The specificities of small molecule inhibitors of the TGFβ and BMP pathways. *Cell Signal.* **23,** 1831–1842 CrossRef
24. Bain, J., Plater, L., Elliott, M., Shpiro, N., Hastie, C. J., McLauchlan, H., Klevernic, I., Arthur, J. S. C., Alessi, D. R., and Cohen, P. (2007) The selectivity of protein kinase inhibitors: a further update. *Biochem. J.* **408,** 297–315 CrossRef Medline
25. Turnham, R. E., and Scott, J. D. (2016) Protein kinase A catalytic subunit isoform PRKACA; history, function and physiology. *Gene* **577,** 101–108 CrossRef Medline
26. Herzig, S., and Shaw, R. J. (2018) AMPK: guardian of metabolism and mitochondrial homeostasis. *Nat. Rev. Mol. Cell Biol.* **19,** 121–135 CrossRef
27. Sanidas, I., Polytarchou, C., Hatziapostolou, M., Ezell, S. A., Kottakis, F., Hu, L., Guo, A., Xie, J., Comb, M. J., Iliopoulos, D., and Tsichlis, P. N. (2014) Phosphoproteomics screen reveals akt isoform-specific signals linking RNA processing to lung cancer. *Mol. Cell* **53,** 577–590 CrossRef Medline
28. Iliopoulos, D., Polytarchou, C., Hatziapostolou, M., Kottakis, F., Maroulakou, I. G., Struhl, K., and Tsichlis, P. N. (2009) MicroRNAs differentially regulated by Akt isoforms control EMT and stem cell renewal in cancer cells. *Sci. Signal.* **2,** ra62 CrossRef
29. Collins, M. P., and Forgac, M. (2018) Regulation of V-ATPase assembly in nutrient sensing and function of V-ATPases in breast cancer metastasis. *Front. Physiol.* **9,** 902 CrossRef Medline
30. Zoncu, R., Bar-Peled, L., Efeyan, A., Wang, S., Sancak, Y., and Sabatini, D. M. (2011) mTORC1 senses lysosomal amino acids through an inside-out mechanism that requires the vacuolar H(+)-ATPase. *Science* **334,** 678–683 CrossRef Medline
31. Dibble, C. C., and Manning, B. D. (2013) Signal integration by mTORC1 coordinates nutrient input with biosynthetic output. *Nat. Cell Biol.* **15,** 555–564 CrossRef Medline
32. Inoue, H., Hase, K., Segawa, A., and Takita, T. (2013) H89 (N-[2-p-bromocinnamylamino-ethyl]-5-isoquinolinesulphonamide) induces autophagy independently of protein kinase A inhibition. *Eur. J. Pharmacol.* **714,** 170–177 CrossRef
33. Zhang, C.-S., Jiang, B., Li, M., Zhu, M., Peng, Y., Zhang, Y.-L., Wu, Y.-Q., Li, T. Y., Liang, Y., Lu, Z., Lian, G., Liu, Q., Guo, H., Yin, Z., Ye, Z., *et al.* (2014) The lysosomal v-ATPase-regulator complex is a common activator for AMPK and mTORC1, acting as a switch between catabolism and anabolism. *Cell Metab.* **20,** 526–540 CrossRef Medline
34. Soliman, M., Seo, J.-Y., Kim, D.-S., Kim, J.-Y., Park, J.-G., Alfajaro, M. M., Baek, Y.-B., Cho, E.-H., Kwon, J., Choi, J.-S., Kang, M.-I., Park, S.-I., and Cho, K.-O. (2018) Activation of PI3K, Akt, and ERK during early rotavirus infection leads to V-ATPase-dependent endosomal acidification required for uncoating. *PLoS Pathog.* **14,** e1006820 CrossRef Medline
35. Matsuda-Lennikov, M., Suizu, F., Hirata, N., Hashimoto, M., Kimura, K., Nagamine, T., Fujioka, Y., Ohba, Y., Iwanaga, T., and Noguchi, M. (2014) Lysosomal interaction of Akt with Phafin2: a critical step in the induction of autophagy. *PLoS ONE* **9,** e79795 CrossRef Medline
36. Hirata, N., Suizu, F., Matsuda-Lennikov, M., Tanaka, T., Edamura, T., Ishigaki, S., Donia, T., Lithanatudom, P., Obuse, C., Iwanaga, T., and Noguchi, M. (2018) Functional characterization of lysosomal interaction of Akt with VRK2. *Oncogene* **37,** 5367–5386 CrossRef
37. Nezu, J., Motojima, K., Tamura, H., and Ohkuma, S. (1992) Molecular cloning of a rat liver cDNA encoding the 16 kDa subunit of vacuolar H(+)-ATPases: organellar and tissue distribution of 16 kDa proteolipids. *J. Biochem.* **112,** 212–219 CrossRef
38. Li, D. L., Wang, Z. V., Ding, G., Tan, W., Luo, X., Criollo, A., Xie, M., Jiang, N., May, H., Kyrychenko, V., Schneider, J. W., Gillette, T. G., and Hill, J. A. (2016) Doxorubicin blocks cardiomyocyte autophagic flux by inhibiting lysosome acidification. *Circulation* **133,** 1668–1687 CrossRef Medline
39. Rao, V. K., Zavala, G., Deb Roy, A., Mains, R. E., and Eipper, B. A. (2019) A pH-sensitive luminal His-cluster promotes interaction of PAM with V-ATPase along the secretory and endocytic pathways of peptidergic cells. *J. Cell. Physiol.* **234,** 8683–8697 CrossRef Medline
40. Ran, F. A., Hsu, P. D., Wright, J., Agarwala, V., Scott, D. A., and Zhang, F. (2013) Genome engineering using the CRISPR-Cas9 system. *Nat. Protoc.* **8,** 2281–2308 CrossRef
41. Toyama, E. Q., Herzig, S., Courchet, J., Lewis, T. L., Losón, O. C., Hellberg, K., Young, N. P., Chen, H., Polleux, F., Chan, D. C., and Shaw, R. J. (2016) Metabolism. AMP-activated protein kinase mediates mitochondrial fission in response to energy stress. *Science* **351,** 275–281 CrossRef
42. Labun, K., Montague, T. G., Gagnon, J. A., Thyme, S. B., and Valen, E. (2016) CHOPCHOP v2: a web tool for the next generation of CRISPR genome engineering. *Nucleic Acids Res.* **44,** W272–W276 CrossRef